J Polym Res (2008) 15:453–458
DOI 10.1007/s10965-008-9191-5

Flame retardant and the degradation mechanism of high impact polystyrene/Fe-montmorillonite nanocomposites

Qinghong Kong · Ruibin Lv · Shijun Zhang

Received: 28 October 2007 / Accepted: 13 March 2008 / Published online: 15 April 2008

Abstract High impact polystyrene/Fe-montmorillonite (HIPS/Fe-MMT) nanocomposites were successfully prepared by melting intercalation. The nanostructures of HIPS/Fe-MMT were testified by X-ray diffraction (XRD) and transmission electron microscope (TEM). Corresponding to pure HIPS, the thermal stability of HIPS/Fe-MMT nanocomposites was notably improved. The peaks of heat release rate (PHRR) and the mass loss rate (MLR) were significantly reduced after the formation of the HIPS/Fe-MMT nanocomposites from cone calorimetry. And nanocomposites PHRR was further lower with the increase of Fe-MMT content in the range of 1 to 5 wt%. The degradation mechanism of HIPS and HIPS/Fe-MMT nanocomposites was conducted by pyrolysis gas chromatography mass spectrometry (Py-GC-MS). And the reason of the enhancement of thermal stability maybe is that structural iron is the operative site for radical trapping in the Fe-MMT and the nanostructure enhances the interaction of the chains of the HIPS.

Keywords Fe-montmorillonite · Py-GC-MS · High impact polystyrene · Melting intercalation · Nanocomposites · Flame retardant

Introduction

Nanocomposites, composed of clay and polymer, have been studied extensively for some time and it has been shown that most of the properties are enhanced in the presence of a small amount of clay. For instance, incorporation of a few percent of clay in many cases increases the modulus, strength, gas barrier properties, and heat stability, compared to the pure polymers [1–4]. These improvements in the properties are the result of the nanometer scale dispersion of clay in the polymer matrix [5, 6]. This space between the clay layers is referred to as the clay gallery. To make compatible with polymers, the sodium ions are usually ion-exchanged with an organic ammonium or phosphonium salt to convert this material into a hydrophobic ammonium or phosphonium treated clay.

High-impact polystyrene (HIPS) is widely used for electrical appliances, electronic instruments and building materials. HIPS are composite material consisting of a PS phase and a dispersed polybutadiene (PB) rubber phase. In this article, the effect of synthetic Fe-montmorillonite (Fe-MMT) in HIPS/Fe-MMT nanocomposites was studied. The structure of the Fe-MMT is the same to that of natural MMT. The difference is that Fe^{3+} ion replaced Al^{3+} ion in the crystal lattice. The clay containing iron was applied to catalytic field many year ago [7, 8], and they perform catalytic activity very well. In the previous research, the structural iron can be the important site of radical trapping [9]. A new application of Fe-MMT in HIPS was proved and some favorable properties compared with pure polymer in this study. The nanocomposites were prepared using this type of organic Fe-montmorillonite (Fe-OMT) by melt intercalation, and the nanostructure, thermal property and fire property were measured.

Experimental

Materials

The majority of chemicals used in this study, including cetyltrimeyhyl ammonium bromide (CTAB). Acidic sodi-

Q. Kong (✉) · R. Lv · S. Zhang
School of the Environment, Jiangsu University,
Zhenjiang, Jiangsu 212013, People's Republic of China
e-mail: kongqh@ujs.edu.cn

um silicate ($Na_2SiO_3.9H_2O$), iron (III) chloride ($FeCl_3.6H_2O$), zinc acetate [Zn $(CH_3COO)_2.2H_2O$] and sodium hydroxide (NaOH) were all from Shanghai Chemistry Company. High impact polystyrene (492J) was supplied as pellets by SAL Petrochemical (Zhangjiagang) Co., Ltd., China.

Preparation of HIPS/Fe-MMT hybrid

The way of the synthesis and modifiability of Fe-MMT was reports in previous thesis [10, 11]. HIPS was melt-mixed with Fe-OMT at 180°C using a twin-roll mill (XK-160, made in Jiangshu, China) for 10 min to yield the hybrid, denoted HIPS/Fe-MMT and the listing order in Table 1.

Characterization

X-ray diffraction (XRD) was used to characterize the layer conformation of Fe-MMT in the composite. The operation parameters were Cu-Kα (λ=1.54178 Å) radiation at a generator voltage of 30 kV and current of 10 mA. The range of the diffraction angle was 2θ=1.5–10°. The structure of the composite was observed by transmission electron microscope (TEM), TEM specimens were cut at room temperature using an ultramicrotome (Ultracut-1, UK) with a diamond knife.

The thermal properties of HIPS and HIPS nanocomposites were investigated by Thermogravimetric analyzed (TGA, TA50). In each case, the 10 mg specimens were heated from 25 to 600 °C at the rate of 10 °C/min under nitrogen flow.

The cone calorimetry experiments were carried out following the procedure defined in ISO 5660, on the 3 mm thick100×100 mm^2 plaques. The cone data obtained are reproducible to within ±10% when measured at 35 kW/m^2 heat flux.

Comparative thermal degradation of HIPS/Fe-MMT and virgin HIPS was conducted by pyrolysis gas chromatography mass spectrometry (Py-GC-MS). The samples were purged for 1 min under 99.999% pure helium flow (100 ml/min) and pyrolyzed at 450 °C in a Frontier Labs pyrolyzer interfaced with a Agilent 6890 GC and Agilent 5970 MSD. The GC column was heated from 50 to 280 °C at 10 °C/min and held at the final temperature for 10 min.

Table 1 Formulations of HIPS composites

Sample code	HIPS (wt%)	Fe-OMT (wt%)
HIPS1	100	0
HIPS2	99	1
HIPS3	97	3
HIPS4	95	5

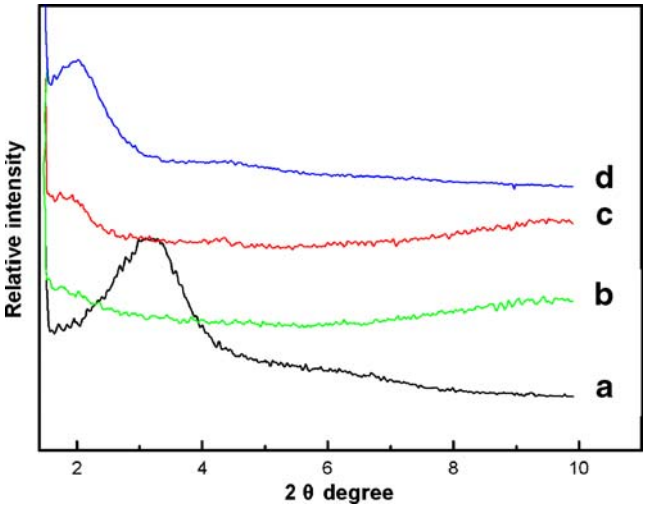

Fig. 1 XRD patterns of HIPS nanocomposites containing different amount of *a* Fe-OMT; *b* HIPS2; *c* HIPS3; *d* HIPS4

Results and discussion

Nanostructure of HIPS/Fe-MMT composites

After the Fe-MMT was modified by CTAB, the original inorganic Fe-MMT (the d_{001} spacing was about 15 Å which was previous report [11]) became hydrophobic and the interlayer galleries were also amplification. The d spacing has changed into 28 Å (Fig. 1a) [11]. Figure 1b–d show a series of XRD patterns of HIPS/Fe-MMT composites containing different amount of Fe-OMT. With the decrease of the Fe-OMT content (from 5 to 1 wt%), the peak relative intensity of the (001) plane became weaker. The strong (001) plane peak of HIPS4 corresponding to d_{001} (about 37 Å; Fig. 1d) was clearly observed, resulting from this kind of composite: intercalated nanocomposites. Along with Fe-OMT content depression, the diffraction peak of (001) plane was weak (Fig. 1c, 3 wt% Fe-OMT), it declared the intercalated-exfoliated nanocomposites was formed. When the content of Fe-OMT was 1 wt%, the peak was disappeared. It declared the exfoliated morphology was formed or the major. When the content of Fe-OMT increased, structures of HIPS/Fe-MMT nanocomposites changed from exfoliation to intercalation.

In order to certify XRD spectrum analysis of the HIPS/Fe-MMT nanostructure, the TEM micrographs of the HIPS/Fe-MMT composites were shown in Fig. 2, where the bright region represented the polymer matrix and the dark narrow stripes represented the Fe-MMT. From TEM micrograph of HIPS2 and HIPS3 (showing Fig. 2a and b respectively), it detected the Fe-MMT was dispersed in the HIPS matrix. The exfoliated state was major in Fig. 2a which most MMT layers were randomly dispersed in the HIPS matrix. In Fig. 2b, it was typical intercalated

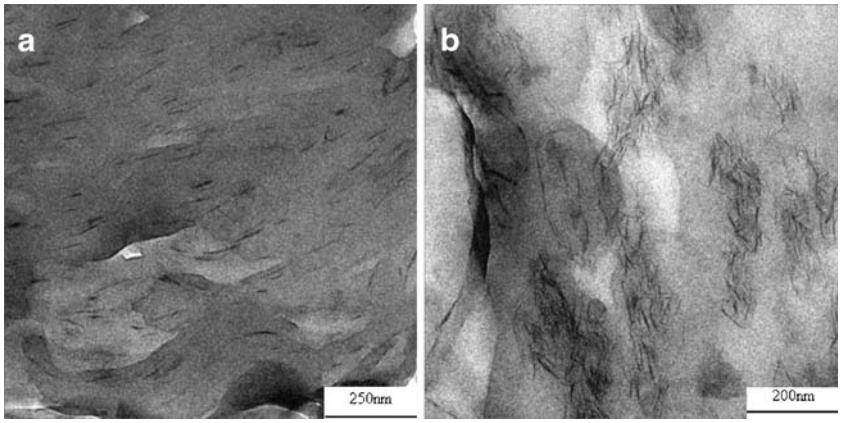

Fig. 2 TEM micrograph of HIPS2 (**a**) and HIPS3 (**b**)

dispersion which the layers of silicate had certain tendency of arrangement; and the minor was exfoliated state. The conclusion was coincident with XRD of the nanocomposites.

Thermal stability of HIPS/Fe-MMT nanocomposites

In the experimental conditions, the thermal decomposition behaviors of pure HIPS, HIPS/Fe-MMT nanocomposites series and Fe-OMT were performed by TGA in Fig. 3 and Table 2. It was seen that the thermal stability of the HIPS/Fe-MMT nanocomposites was noticeably improved contrasting to that of the HIPS matrix. The data of the onset of the degradation temperatures (at which 10% degradation occurs, symbol $T_{0.1}$), the midpoint of the degradation temperatures (at which 50% degradation occurs, symbol $T_{0.5}$) and the residue that was at 600 °C, were shifted to higher with enhancing the Fe-OMT content in the HIPS/Fe-MMT nanocomposites contrasting to that of HIPS. The temperature of decomposition was increased as much as 20–30 °C. The origin of the noticeable increased in the temperature of decomposition mainly resulted from strong interaction between polymer and clay [12]. Polymer chains subjected to the silicate layers. Surface features of silicate layers made many polymer chains extremes link the same silicate layers. So those layers acted as cross-bonding points. In the Table 2, HIPS4 (5 wt% Fe-OMT) had the highest thermal property of the three types of nanocomposites. Thermal decomposition of the Fe-OMT takes place at around 200 °C and proceeds according to the Hofmann degradation mechanism [11–13]. The course was similar to the Na-OMT, and it was described in our previous report.

The fire performance of nanocomposites

Under fire like conditions, using the cone calorimeter has revealed improved flammability properties for many types of polymer/clay nanocomposites [14, 15]. The cone calorimetric results for HIPS/Fe-MMT series nanocomposites and pure HIPS were shown in Fig. 4. It was found that nanocomposites had a much lower peak heat release rate (PHRR) than that of the virgin polymer. The reduction of PHRR in nanocomposites improved as the content of Fe-OMT increased. The PHRR of HIPS/Fe-MMT nanocomposites (with Fe-OMT loading 1, 3, 5 wt%) were 29%, 36%, and 52% lower than that of pure HIPS, respectively. The PHRR fell as the amount of Fe-OMT increases. In

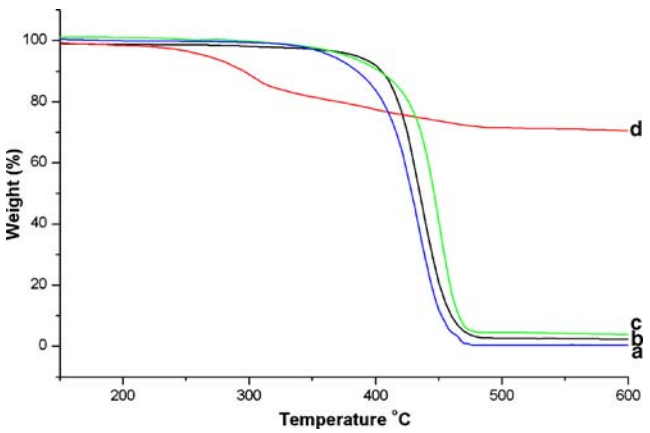

Fig. 3 Fe-OMT, pure HIPS and HIPS/Fe-MMT nanocomposites characterized by TGA *a* HIPS1; *b* HIPS2; *c* HIPS3; *d* Fe-OMT

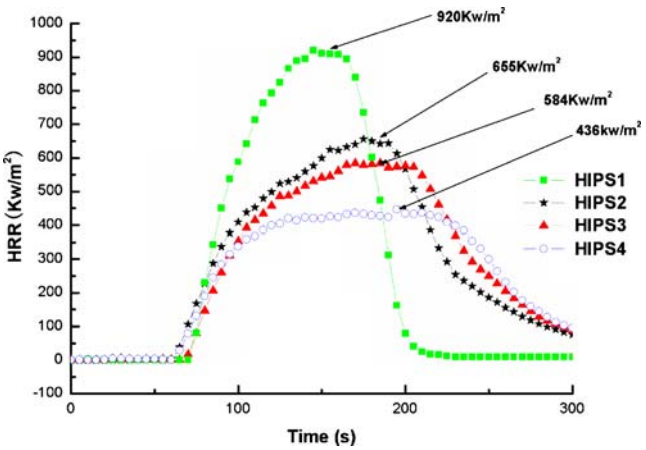

Fig. 4 Peak heat release rates for HIPS and HIPS/Fe-MMT nanocomposites

Table 2 TGA results of HIPS/Fe-MMT nanocomposites and Fe-OMT

Sample code	$T_{0.1}$ (°C)	$T_{0.5}$ (°C)	Residue at 600 °C (wt%)
HIPS1	385.8	428.4	0.09
HIPS2	403.3	435.6	1.42
HIPS3	405.8	446.1	3.35
HIPS4	412.3	448.3	5.45
Fe-OMT	283.6	/	70.07

addition to measuring PHRR, the cone calorimeter also measures other fire-relevant properties such as mass loss (ML) and mass loss rate (MLR; Figs. 5 and 6). Comparison with PHRR data in Fig. 6, the MLR of nanocomposites showed a similar decrease to that of pure polymer, which revealed that the nano-dispersed MMT reduced the PHRR by reducing the MLR (fuel feed rate) of the nanocomposites. This was consistent with the reports by Gilman [14]. These results indicated that an intercalated material was more effective than an exfoliated material in flame retardancy. Wilkie had reported the similar result in polystyrene (PS)/clay nanocomposites [16]. The suggested mechanism by which clay nanocomposites function involved the formation of a char that serves as a barrier to both mass and energy transport [16]. It was reasonable that as the fraction of clay increases, the amount of char that can be formed increases and the rate at which heat was decreased. The other reasons maybe was the presence of structural iron in Fe-MMT [9]. The burning of polymer was the reaction of free radical chain [9, 17]. Structural iron was the operative site for radical trapping within the clay in the course of polymer nanocomposites burning.

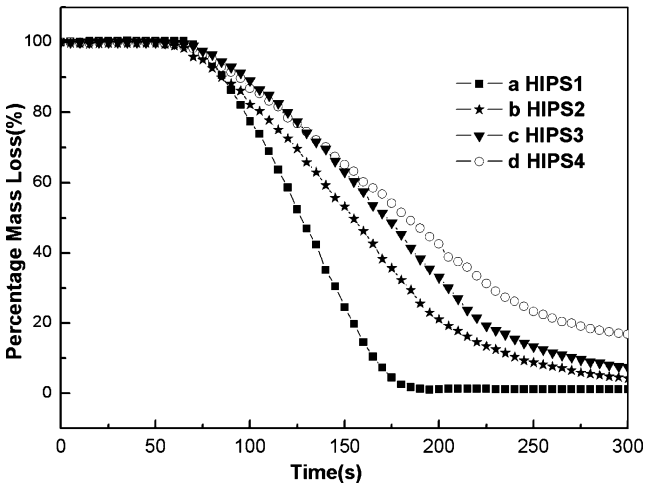

Fig. 5 Mass loss (*ML*) data for pure HIPS and HIPS/Fe-MMT nanocomposites

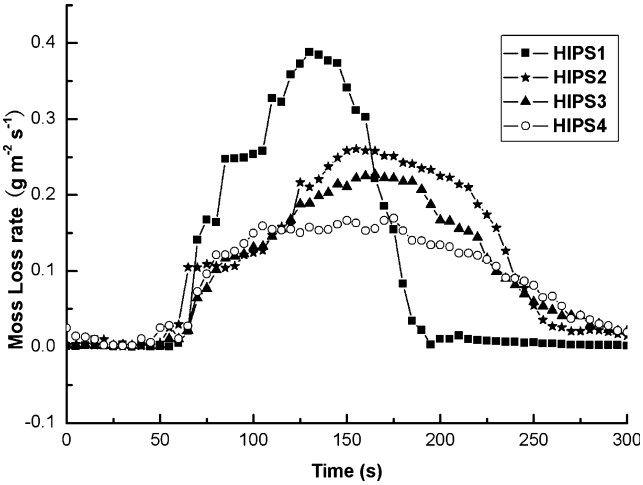

Fig. 6 Mass loss rate (*MLR*) data for pure HIPS and HIPS/Fe-MMT nanocomposites

The degradation mechanism analysis by Py-GC-MS

In order to investigate the difference the degradation mechanism between of HIPS and HIPS/Fe-MMT nanocomposites, the pyrolysis gas chromatography of HIPS1 and HIPS4 samples was shown in Fig. 7. The chemical structure of the main crackates in Fig. 7 was offered in Table 3. For virgin HIPS, the three major peaks at retention times of 3.96, 14.61, and 22.26 min had yielded mass spectra that, according to the Wiley database, are respectively consistent with styrene monomer, 2, 4-diphenylbut-1-ene (dimmer) and 2, 4, 6-triphenylhex-1-ene (trimer) [18, 19]. The two minor peaks at retention times of 1.71 and 4.98 min were consistent with butadiene and α-methylstyrene. It suggested that abundant product was styrene, which was formed by β-scission of a chain-end radical (unzipping). Intermolecular radical transfer yielded trace amounts of α-methylstyrene [20]. The pyrogram for the HIPS/Fe-MMT system was more complex compared with virgin HIPS. And the distinct difference was the peak whose mass spectrum had been matched with that of α-methylstyrene. Its abundance was about 22.1% of that for styrene in HIPS4. Then the abundance of α-methylstyrene was about 4.4% of that for styrene in HIPS1. This was high compared with the trace amounts of α-methylstyrene produced by the degradation of virgin HIPS. The HIPS4 showed an unusually high yield of α-methylstyrene that indicated intensification of intermolecular radical transfer reactions [19]. Jang and Wilkie [21] thought that the primary radical was transformed to the tertiary radical because of its increased stability, leading to the formation of α-methylstyrene via β-scission and the formation of another secondary radical, after the formation of primary and secondary radicals via chain scission, the schematic figure of β cracking was shown in Fig. 8. The key in this mechanism was hydrogen transfer

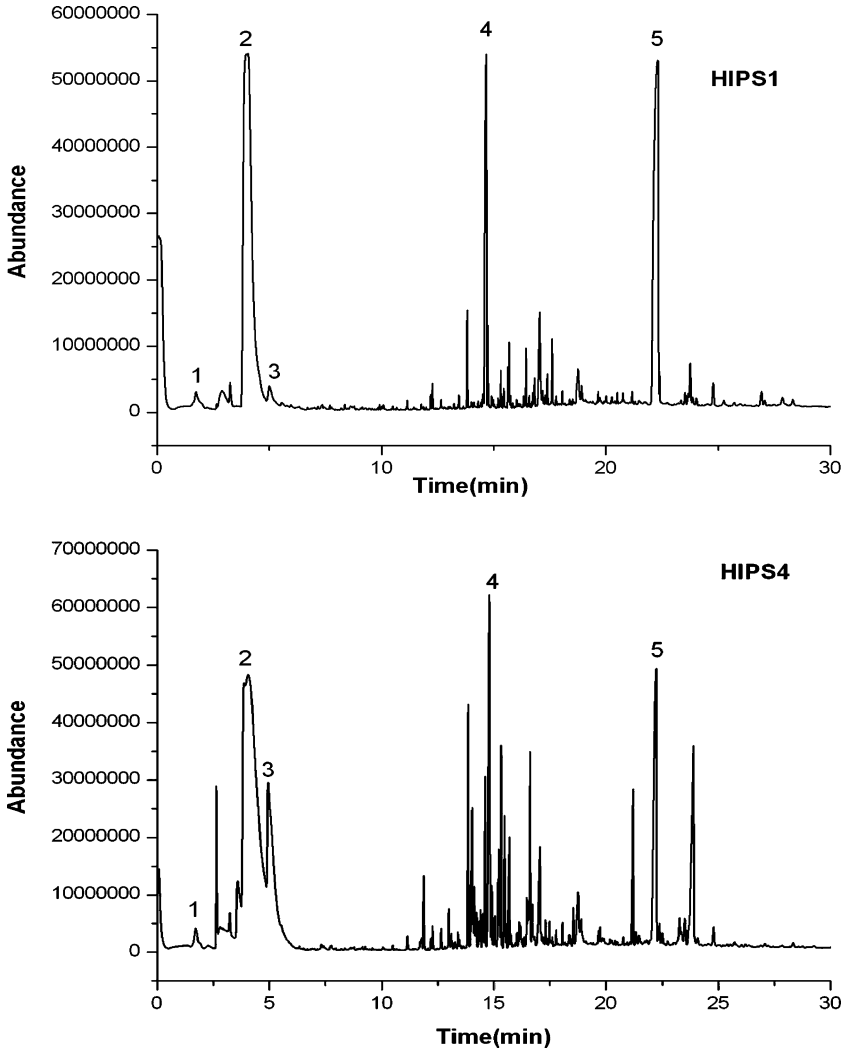

Fig. 7 GC pyrograms of virgin HIPS and HIPS4 nanocomposites pyrolyzed at 450 °C: *1*, butadiene; *2*, styrene; *3*, α-methylstyrene; *4*, 2, 4-diphenylbut-1-ene (dimmer); *5*, 2, 4, 6-triphenylhex-1-ene (trimer)

Table 3 The chemical structures of compounds corresponding to the major peaks in GC chromatograms in Fig. 7

No.	m/z	compounds	Chemical formula
1	54	butadiene	
2	91	styrene	
3	118	α-methylstyrene	
4	145	2, 4-diphenylbut-1-ene	
5	196	2, 4, 6-triphenylhex-1-ene	

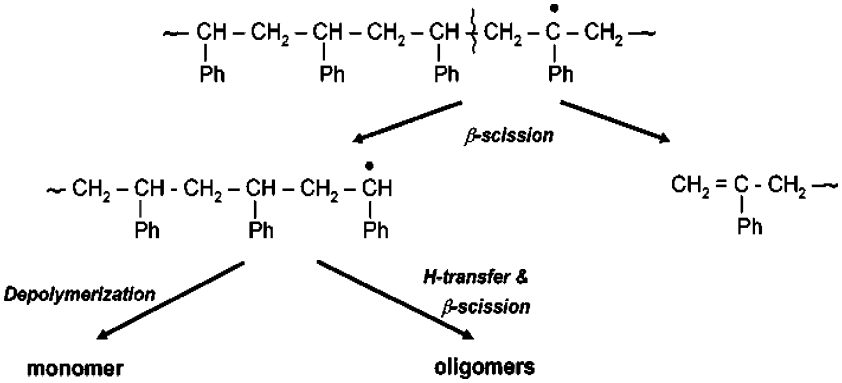

Fig. 8 Schematic figures of β cracking

from one chain to another, and yielded a mid-chain radical. An unsaturated chain end was produced when the mid-chain radical was cracking. β-scission of the latter yielded α-methylstyrene radical which converted into α-methylstyrene by hydrogen abstraction. Chen and Vyazovkin [19] had reported the brush mechanism model in degradation mechanism of polystyrene/clay nanocomposites was expounded. The brush hypothetical model had been outlined that links the enhancement of intermolecular interactions to the formation. The chain conformation for random coils of pure HIPS cannot interact with others. When the nanocomposites were formed via melting, the chains of HIPS were limited by the layers of the Fe-MMT, the interchain distance was decreased and maybe the interaction between chains increased. So the linear chain should increase the probability of intermolecular reactions and the yield of α-methylstyrene was high in the HIPS4. And the structural iron strengthened this effect further and the structural iron was the operative site for radical trapping within the clay [9].

Conclusions

HIPS/Fe-MMT nanocomposites were successfully prepared via melting intercalation. The thermal stability of HIPS/Fe-MMT nanocomposites improved observably in comparison with HIPS. The peak heat release rate (PHRR) and the mass loss rate (MLR) from cone calorimetry of the nanocomposites were significantly reduced compared with that of the virgin HIPS. And from the results of Py-GC-MS, the HIPS/Fe-MMT nanocomposites system showed an unusually high yield of α-methylstyrene that indicated intensification of intermolecular radical transfer reactions. In conclusion, the unique properties of the nanocomposites result from the strong interactions between the silicate structural layers and the polymeric chains and the iron maybe have the important site of radical trapping.

Acknowledgment The work was financially supported by start fund for advanced professional of Jiangsu University (No.07JDG017). The authors would like to express their sincere thanks to State Key Laboratory of Fire Science (University of Science and Technology of China).

References

1. Okada A, Kawasuni M et al (1987) Polym Prepr 28:47
2. Kim YK, Choi YS, Wang MH, Chung IJ (2002) Chem Mater 14 (12):4990–4995
3. Vaia RA, Jandt KD, Giannelis EP (1996) Chem Mater 8 (11):2628–2635
4. Celik M, Onal M (2007) J Polym Res 14(4):313–317
5. Chiu FC, Chu PH (2006) J Polym Res 13(1):73–78
6. Zhu J, Wilkie CA (2000) Polym Int 49:1158–1163
7. Rightor EG, Tzou MS, Pinnavaia TJ (1991) J Catal 130(1):29–40
8. Ding Z, Kloprgge JT, Frost RL, Lu GQ (2001) J Porous Mater 8 (4):273–293
9. Zhu J, Morgan AB, Wilkie CA (2001) Chem Mater 13(12):4649–4654
10. Nagase T, Iwasaka T, Onodera Y, Dutta NC (1999) Chem Lett 4:303–304
11. Kong QH, Hu Y (2006) Polym Adv Technol 17:463–467
12. Gilman JW, Kashiagi T (2000) In: Pinnavaia TJ, Beall GW (eds) Polymer-clay nanocomposites. Wiley, New York, p 193
13. Xie W, Gao ZM, Pan WP, Vaia R (2001) Chem Mater 13 (9):2979–2990
14. Gilman JW, Jackson CL, Morgan AB, Harris R, Manias E, Giannelis EP, Wuthenow M, Hilton D, Phillips SH (2000) Chem Mater 12(7):1866–1873
15. Zanetti M, Kashiwagi T, Falqui L, Camino G (2002) Chem Mater 14:881–887
16. Zhu J, Morgan AB, Lamelas FJ, Wilkie CA (2001) Chem Mater 13:3774–3780
17. Ou YX, Chen Y et al (2001) Flame-retarded polymeric material. National Defence Industry Press, Beijing, pp 13–15
18. Grassie N, Scott G (1985) Polymer degradation and stabilization. Cambridge University Press, Cambridge
19. Chen K, Vyazovkin S (2005) Macromol Rapid Commun 26 (9):690–695
20. Lehrle RS, Pattenden CS (1999) Polym Degrad Stab 63(1):153–158
21. Jang BN, Wilkie CA (2005) Polymer 46(9):2933–2942